

Self-Assembly-Induced Supramolecular Hexagonal Columnar Liquid Crystalline Phase Using Laterally Attached Nonmesogenic Templates

Huilin Tu,[†] Xinhua Wan,[†] Yuxiang Liu,[†] Xiaofang Chen,[†] Dong Zhang,[†] Qi-Feng Zhou,^{*,†} Zhihao Shen,[‡] Jason J. Ge,[‡] Shi Jin,[‡] and Stephen Z. D. Cheng^{*,†,‡}

Department of Polymer Science and Engineering, College of Chemistry, Peking University, Peking, China, and Maurice Morton Institute and Department of Polymer Science, The University of Akron, Akron, Ohio 44325-3909

Received October 22, 1999; Revised Manuscript Received June 14, 2000

ABSTRACT: A novel poly[di(4-heptyl) vinylterephthalate] has been synthesized based upon a free radical polymerization from a newly designed monomer having a nonmesogenic template with two double-swallow-tailed 4-heptyl (Y-shaped) groups. The resulting polymer consists of a polyethylene backbone and a 2,5-bis(4-heptyloxycarbonyl)phenyl lateral substituent on every second carbon atom of the backbone. Although neither the backbone nor the pendent template exhibits liquid crystalline (LC) behavior, they couple together to form a supramolecular hexagonal columnar LC phase on a scale of greater than 1.5 nm in the polymer. Therefore, it is deduced that this supramolecular LC structure is constructed via a cooperative assembly of a helical arrangement of the backbones with the pendent templates.

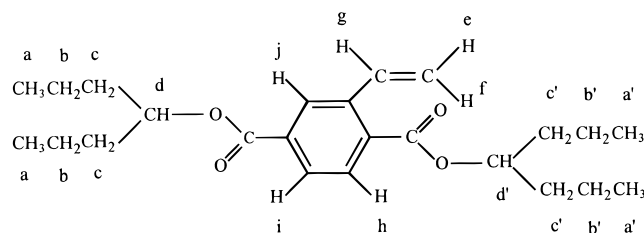
Introduction

Thermotropic liquid crystalline (LC) polymers commonly possess mesogenic groups which have an anisotropic geometry, such as rigid rods or disks, in addition to specific molecular interactions.¹ These mesogenic groups play a critical role in forming LC polymers when they are covalently incorporated into either the side chains or the main-chain backbones of polymers.^{2,3} In traditional understanding, the mesogenic groups must consist of two or more 1,4-phenylenes directly linked together or through linkages such as ester, oxymethylene, or methylene units. In some cases, the 1,4-cyclohexyl ring or 2,5-disubstituted-1,3-dioxane is also used to replace one of the phenylenes.⁴

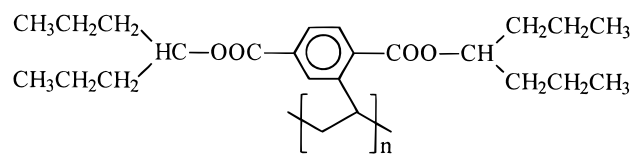
For side-chain LC polymers, two categories can be distinguished on the basis of the type of attachment of the side-chain LC mesogens to the backbone chains: terminally and laterally attached.^{4–6} Since the laterally attached mesogens are generally much larger in size than the repeat units of the polymer backbones, the substituted mesogens force the backbone into a somewhat extended helical conformation. This, in turn, allows the mesogens in the side chains to jacket around the backbones to form a cylinder.^{7–10} Low ordered LC phases, such as nematic (N), smectic A (S_A), and smectic C (S_C) phases, have been identified in laterally attached LC polymers.^{11–13} It is interesting to ask whether the side-chain nonmesogenic templates which possess a large enough stereo-hindrance can stabilize mesophase structures. In a recent study of laterally attached polymers, stable mesophases have been observed when the side-chain templates contain dicyclohexyl vinylterephthalates in which only one 1,4-phenylene group was linked to two 1,4-cyclohexyl rings through ester groups (a vinyl group was attached to this phenylene group for polymerization).^{14,15} The side-chain templates alone melt at –30 °C and directly enter the isotropic liquid without passing through any LC phases. It has

been deduced that the LC phase formed in these polymers must be constructed via a supramolecular assembly, as compared to normal LC phases, which are formed by molecular packing. A similar observation has also been found in a series of poly[di(cycloalkyl) vinylterephthalate]s.¹⁶

In this study, we report on the synthesis and structural characterization of poly[di(4-heptyl) vinylterephthalate]. This polymer consists of a polyethylene backbone and a 2,5-bis(4-heptyloxycarbonyl)phenyl template laterally substituted on every second carbon atom of the backbone. The monomer chemical structure is



and the corresponding polymer chemical structure is



It is interesting that in each side-chain template only one phenylene group connects with two double-swallow-tailed 4-heptyl (Y-shaped) groups via an ester linkage. Therefore, this template is less rigid than similar structures used in previous work.^{14–16} On the basis of our structural analyses, this polymer shows a supramolecular hexagonal columnar LC phase on a nanometer length scale by the self-assembled nonmesogenic templates which are jacketed onto the backbones. However, no long-range ordered structures are found in the molecular packing on a length scale of around 0.5 nm.

[†] College of Chemistry, Peking University.

[‡] The University of Akron.

* To whom the correspondence should be addressed.

Experimental Section

Monomer and Polymer Synthesis. A monomer, di(4-heptyl) vinylterephthalate, was synthesized from 4-heptanol and vinylterephthalic acid through the phosphorylation reaction with a yield of 65%. The product was a colorless isotropic liquid at room temperature. The chemical structure was confirmed using mass spectroscopy (MS, VG-ZAB-HS), proton nuclear magnetic resonance (^1H NMR, Bruker ARX 400, solvent CDCl_3), and infrared spectroscopy (FTIR, Bruker Vector 22 FTIR). Mass spectra show that $m/e = 388$ (parent), 175 (base), 290, 273, 147, 130, and 98. ^1H NMR spectra provide chemical shifts of 0.92–0.97 (m, 12H, H_a , H_a'), 1.38–1.43 (m, 8H, H_b , H_b'), 1.66–1.73 (m, 8H, H_c , H_c'), 5.16–5.22 (m, 2H, H_d , H_d'), 5.41–5.79 (dd, 1H, H_e , $J_{ef} = 1.0$ Hz, $J_{eg} = 11.0$ Hz), 5.74–5.79 (dd, 1H, H_f , $J_{ef} = 1.0$ Hz, $J_{fg} = 17.4$ Hz), 7.39–7.47 (q, 1H, H_g , $J_{eg} = 11.0$ Hz, $J_{fg} = 17.5$ Hz), 7.88–7.90 (d, 1H, H_h , $J_{hi} = 8.1$ Hz), 7.95–7.98 (dd, 1H, H_i , $J_{hi} = 8.1$ Hz, $J_{ij} = 1.6$ Hz), and 8.25 (d, 1H, H_j , $J_{ij} = 1.6$ Hz). FTIR spectra show the vibration bands of 1245 cm^{-1} (C–O–C), 1717 cm^{-1} (C=O), 2960 cm^{-1} (CH_3 , ν_{as}), 2874 cm^{-1} (CH_3 , ν_{s}), and 2933 cm^{-1} (CH_2 , ν_{as}).

The polymer was obtained through solution polymerization. The reaction was carried out in tetrahydrofuran (THF) at $60\text{ }^\circ\text{C}$ for 3 days, using 0.5% equivalent moles of azobis(isobutyronitrile) (AIBN) as initiators. The polymer was precipitated in methanol and washed five times. Before further characterization was performed, the polymer was dried in a vacuum over P_2O_5 at $70\text{ }^\circ\text{C}$ for 24 h. The number-average molecular weight and polydispersity of the polymer were 1.0×10^4 and 2.2, respectively (Waters 2410 RI detector, three Waters Styragel columns HT2 + HT3 + HT4, polystyrene as standard and THF as eluant at a flow rate of 1.0 mL/min). Thermogravimetric analysis (at a heating rate of $20\text{ }^\circ\text{C/min}$ in dry nitrogen) showed that the polymer has 1% and 5% weight loss at 281 and $308\text{ }^\circ\text{C}$, respectively.

Equipment and Experiments. In addition to equipment used in the molecular analysis as described in the monomer and polymer synthesis, differential scanning calorimetry (DSC), wide-angle X-ray diffraction (WAXD), and polarized optical microscopy (PLM) were applied to characterize structure and morphology of the polymer. The thermal transitions were detected using a Perkin-Elmer DSC-7. The temperature and heat flow were calibrated using standard materials at different cooling and heating rates between 5 and $40\text{ }^\circ\text{C/min}$. Samples with a typical mass of 10 mg were encapsulated in sealed aluminum pans. A controlled cooling experiment was always carried out first, and a subsequent heating was performed at a rate that was equal to the prior cooling rate.

WAXD powder experiments were performed with a Rigaku 12 kW rotating anode generator (Cu $\text{K}\alpha$ radiation) equipped with a Geigerflex D/max-RB diffractometer. A hot stage in conjunction with the diffractometer was used to study the structural evolution with changing temperature at constant heating and cooling rates. The temperature was controlled within $\pm 1\text{ }^\circ\text{C}$. Films having a thickness of approximately 0.1 mm were mounted on aluminum sheets, and the diffraction patterns were collected by a reflection mode. Samples were scanned in a 2θ range between 2° and 30° . Background scattering was recorded and subtracted from WAXD patterns. To understand the dimensionality of structure order, fiber samples were used to obtain WAXD fiber patterns. Fibers were drawn from the melt and quenched to room temperature. A typical fiber diameter was $30\text{ }\mu\text{m}$. The fibers were annealed at $120\text{ }^\circ\text{C}$ for 48 h. The WAXD fiber patterns were recorded at room temperature for different exposure times using an imaging plate equipped with an 18 kW X-ray rotating anode generator (Cu $\text{K}\alpha$ radiation, Rigaku automated X-ray imaging system with 1500×1500 pixel resolution). The air scattering was subtracted from the WAXD patterns.

Phase morphology was examined via a polarized light microscope (PLM) (Olympus BH-2) coupled with a Mettler hot stage (FP-90). The film thickness was controlled to $10\text{ }\mu\text{m}$, prepared by a solution-cast method. The thermal history was identical to the DSC and WAXD experiments. To confirm the

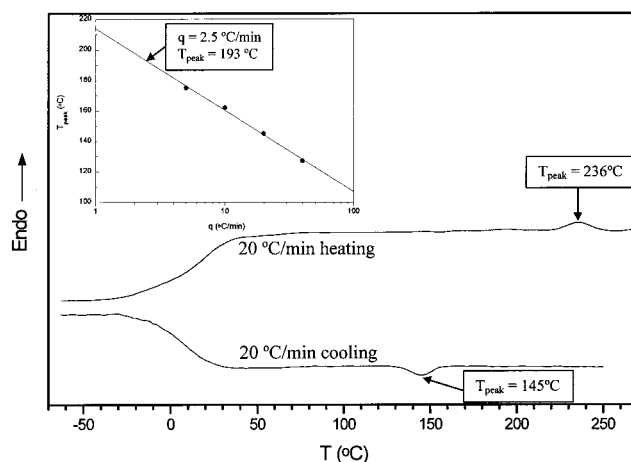


Figure 1. Two DSC thermal diagrams of the polymer during cooling and subsequent heating at $20\text{ }^\circ\text{C/min}$. The inset in this figure is an extrapolation of the transition temperature with respect to the logarithmic cooling rates.

existence of the LC phase, mechanically sheared samples were also examined under PLM.

For monitoring the chemical group orientation in the oriented samples, polarized FT-IR experiments of the mechanically sheared films (at $160\text{ }^\circ\text{C}$ on a KBr substrate) were also conducted on a Mattson Galaxy Series FT-IR 5000 spectrometer equipped with a He:neon laser source and a polarizer rotation stage in a transmission geometry. The accuracy of the wavenumber is within 4 cm^{-1} . A rotation stage was used to control the sample orientation with respect to the polarized IR beam. The rotating range can be between 0° and 90° with an angular accuracy of $\pm 0.5^\circ$ in the azimuthal direction. The calculation of dichroic ratio (A_{\parallel}/A_{\perp}) was carried out using the ratio of intensities obtained between parallel (0°) and perpendicular (90°) spectra of the shear direction with respect to the polarized direction.

Peak deconvolution of overlapped components was conducted using a commercial package of OPUS 2.2 IR/Raman analysis software from Bruker Optics. The peak shape used was based upon a simple mixture of Lorentz functions with local least-squares algorithm. This program had the capability of adjusting parameters to describe the band position, shape, and intensity. Relative intensity was calculated as the integration of individual deconvoluted peaks. The peak fitting procedure was similar to that reported in refs 17 and 18.

Results and Discussion

Figure 1 shows DSC thermal diagrams on both cooling and subsequent heating at a rate of $20\text{ }^\circ\text{C/min}$ as an example. Upon cooling, an exothermic peak can be found at $145\text{ }^\circ\text{C}$, while during subsequent heating, an endothermic process with a peak temperature of $236\text{ }^\circ\text{C}$ is observed. An interesting feature of this observation is that the heats of transition of both exothermic and endothermic processes are identical and small ($0.25 \pm 0.05\text{ kJ/mol}$). This enthalpy change is obviously much smaller than conventional heats of transitions between low ordered N, S_A , or S_C phase and the isotropic melt.^{19–21} It may imply that if this thermal event is associated with an order–disorder transition, this transition must be associated with a small change of molecular interactions (an enthalpy term), which can be detected by DSC. However, it is possible that this transition possess a dominant entropy change. Commonly, this type of order–disorder transitions is attributed to the supramolecular structure change such as in colloid and block copolymer systems.^{20–22} A glass

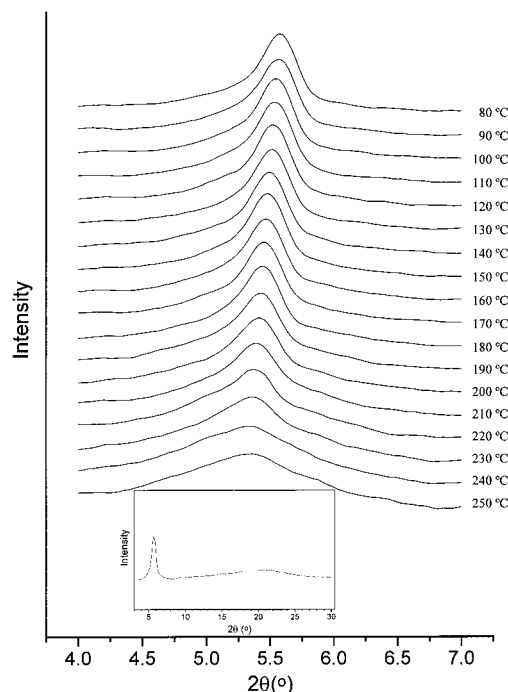


Figure 2. Set of WAXD experimental results in the low-angle region for the polymer during cooling at a rate of 2.5 °C/min. The inset shows a complete scan in a 2θ range of 2°–30°.

transition temperature of this polymer can also be identified at approximately 10 °C as shown in Figure 1.

Of particular interest is that the peak temperature of the exothermic process is cooling rate dependent, but its enthalpy change remains almost constant. As shown in the inset of Figure 1, a plot between the exothermic peak temperature and logarithmic cooling rates indicates that an extrapolation leads to a transition temperature of 193 °C at a cooling rate of 2.5 °C/min. Such a large undercooling dependence of this transition during cooling may represent a relaxation hysteresis during the supramolecular structural formation which is associated with a cooperative dynamics of the templates. However, DSC experiments alone cannot render us the structural change information during this phase transition.

In Figure 2, the WAXD powder patterns of this polymer exhibit an intense diffraction peak at $2\theta = 5.60^\circ$ (d -spacing of 1.58 nm) below 195 °C during cooling at 2.5 °C/min. With further decreasing temperature, this diffraction peak gradually shifts to higher 2θ values due to thermal shrinking. Between 235 and 195 °C, a scattering halo can be found. This halo indicates that in this temperature region only a short-range order exists on the scale of supramolecular length scale. In the wide-angle region of $2\theta > 12^\circ$, no Bragg diffraction can be observed (as shown in the inset of Figure 2, which was recorded at room temperature). Only a diffuse halo can be recognized which has a center position at $2\theta = 21.5^\circ$. This reflects that no long-range ordered crystalline structure formed via molecular packing can be detected on a scale of 0.5 nm over the entire temperature region studied.

Figure 3 shows two plots regarding the diffraction at $2\theta = 5.60^\circ$. The first plot represents a relationship between the reciprocal peak intensity (I^{-1}) and reciprocal temperature (T^{-1}), and the second is a relationship between the full width at half-height (fwhh) and temperature (T). Quantitative analyses of both sets of

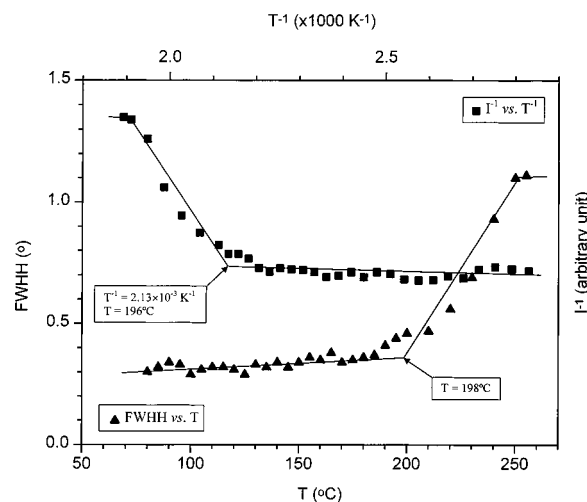


Figure 3. Relationships between the reciprocal intensity (and full width at half-height) of the low-angle reflection with respect to reciprocal temperature (and temperature).

experimental data indicate that during cooling both the I^{-1} and fwhh exhibit sudden changes at 198 °C. Further decreasing the temperature to room temperature had no effect on these two quantities. The discontinuous changes of both quantities of I^{-1} and fwhh at around 195 °C represent a characteristic feature of a first-order transition. This indicates that below 195 °C the polymer does possess a long-range ordered structure on a scale of larger than 1.5 nm.

The I and fwhh of this $2\theta = 5.60^\circ$ diffraction are completely reproducible in multiple heating and cooling cycles. When the cooling rate is slow (such as at 2.5 °C/min), the occurrence of the transition temperature during cooling is close to that observed upon heating. However, as the cooling rate increases, the appearance of this diffraction peak shifts toward lower temperatures which can be seen in the DSC results as shown in the inset in Figure 1. Since no long-range order exists on a scale of less than 0.5 nm in this polymer, the diffraction of $2\theta = 5.60^\circ$ must represent a supramolecular ordered phase constructed by self-assembling entire molecules via laterally attached templates having double-swallow-tailed nonmesogens. However, WAXD powder patterns do not provide structural dimensionality.

The order and symmetry of this self-assembled supramolecular phase can be determined by WAXD fiber analyses as shown in Figures 4. In the region of $2\theta < 12^\circ$, the WAXD pattern shows at least three pairs of sharp diffraction spots on the equator, which represent a long-range periodic arrangement along the direction perpendicular to the fiber axis. The d -spacing value of the pair of diffraction arcs having the lowest 2θ is 1.58 nm, which is identical to the d -spacing of the diffraction at $2\theta = 5.60^\circ$ observed in the WAXD powder pattern (Figure 2). Two additional diffraction arcs on the equator can also be observed at $2\theta = 9.64^\circ$ (d -spacing of 0.917 nm) and 11.12° (d -spacing of 0.795 nm) in Figure 4. The ratios of these two d -spacing ratios with respect to the lowest angle diffraction at $2\theta = 5.60^\circ$ are $1:1/\sqrt{3}:1/\sqrt{4}$, indicating that this supramolecular structure may possess a hexagonal packing along the lateral direction perpendicular to the fiber axis. These diffraction arcs can thus be assigned to be the (100), (110), and (200) planes, respectively. However, it is surprising that a pair of diffuse halos at $2\theta = 21.5^\circ$ (d -spacing of 0.415 nm) is observed on the meridian, suggesting that the structure

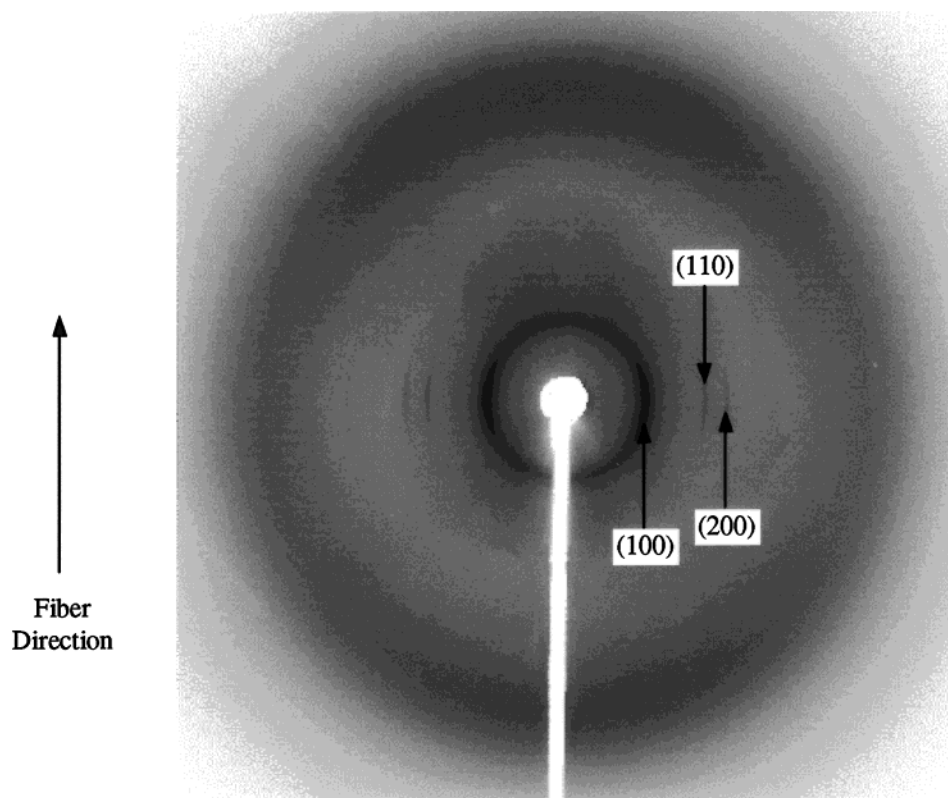


Figure 4. A WAXD fiber pattern of the polymer recorded at room temperature. The fiber direction is along the meridian direction. Three reflections can be observed on the equator. They are (100), (110), and (200) in a hexagonal lattice.

along the fiber direction is disordered. Therefore, a two-dimensional hexagonal columnar packing with $a = b = 1.824$ nm and $\gamma = 120^\circ$ can be determined.

Two possible explanations may account for the origin of the pair of the diffuse halos found at $2\theta = 21.5^\circ$ on the meridian. They may be attributed to either the average distance between neighboring amorphous chains, which are mainly perpendicular to the c -axis, or a periodicity having a short-range order along the c -axis. For the first explanation, note that the average distance between neighboring chains in amorphous polyethylene is at $2\theta = 19.5^\circ$, which corresponds to a d -spacing of 0.455 nm. This is one of the smallest average distances among polymers. Compared with the d -spacing of 0.415 nm for this polymer, it is unreasonable to assume that this pair of halos is attributed to the average distance between neighboring chains along the c -axis. For the second explanation that the periodicity along the c -axis has a short-range order, two speculations need to be discussed. Let us assume that the side-chain templates are only slightly tilted with respect to the ab -plane; i.e., they are more or less perpendicular to the c -axis in the oriented samples. (This assumption will be further discussed in our polarized FTIR experiments; see below.) For the first speculation, one may consider that the backbones are in a zigzag trans conformation, and therefore, the neighboring two side-chain templates must possess a distance of 0.254 nm (since the length of each ethylene unit is 0.254 nm). It is evident that the d -spacing of 0.415 nm is not simply related to a multiple integral of 0.254 nm. Furthermore, the density based on this assumed packing using the zigzag backbone conformation along the c -axis and a single chain occupation in the volume of $ab(\sin 60^\circ)$ is 0.88 g/cm³, which is much lower than the observed experimental data (1.06 g/cm³).

An alternative speculation could be that the short-range ordered periodicity of 0.415 nm is attributed to an average distance of the laterally attached templates which are arranged along the backbone having a helical conformation. It is well-known that for vinyl polymer conformations a larger size pendent group leads to a more open helical conformation.²³ Consequently, this halo may be attributed to periodicity of a helical conformation with the large side-chain templates which may range from $2^{*}4/1$ to $2^{*}6/1$. The calculated helical chain repeat length of the polymer along the c -axis is thus 0.83 and 1.25 nm, respectively, for both the helical conformations. On the other hand, for the lateral packing among the molecules, each polyethylene backbone surrounded by the laterally attached templates with double-swallow tails possesses a periodicity of $a = b = 1.824$ nm in the hexagonal lattice. If we use a calculated side-chain template length of around 1.92 nm (assuming that all the methylene units are in the trans conformation), the side-chain templates need to be tilted 18° away from the ab -plane to accommodate this packing into a hexagonal lattice (1.824 nm). This angle should serve as an upper limit of the tilting for the templates with respect to the ab -plane. For the backbones, the ratio between the c -axis dimension of the helical conformations and the extended repeat unit length (all-trans conformation) can be calculated as 0.817. The calculated density from this helical packing is 1.08 g/cm³, which fits well with the experimental data.

A schematic drawing of the supramolecular packing model is shown in Figure 5a. The center cores are comprised of the helical polyethylene backbones, and the shaded areas are slightly tilted pendent phenylenes and ester groups. The open areas represent the swallow-tailed 4-heptyl groups, which assemble regularly along the polyethylene helical backbones to construct a su-

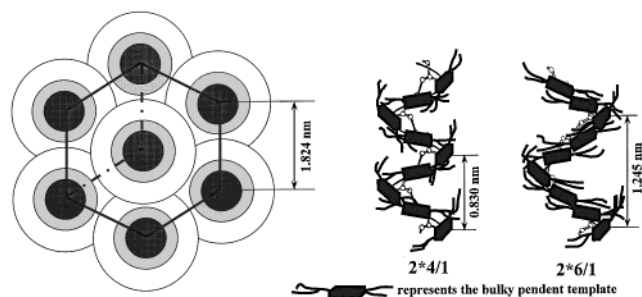


Figure 5. Schematic drawing of the supramolecular hexagonal packing model (a, left) and possible 2*4/1 and 2*6/1 helical chain conformations in the hexagonal packing (b, right).

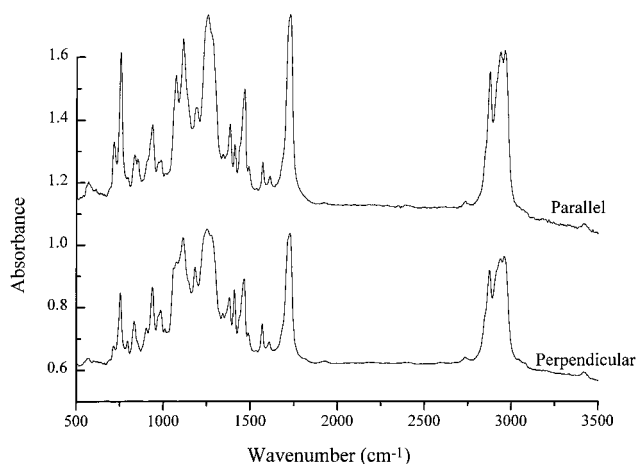
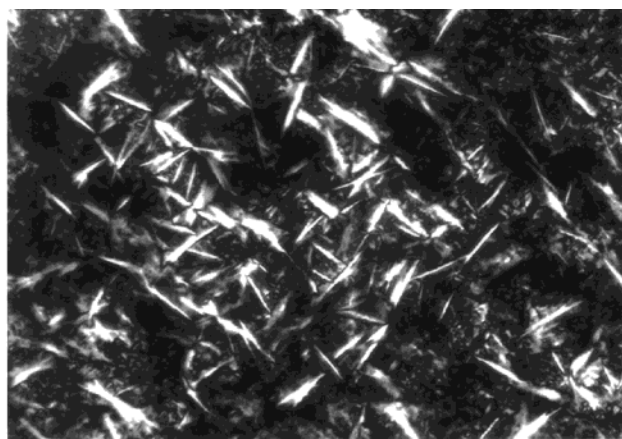


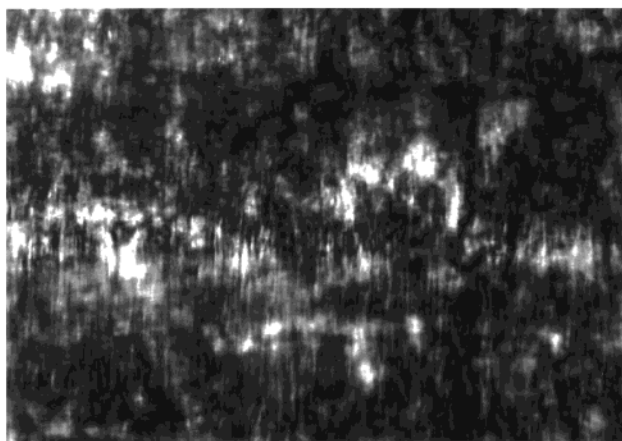
Figure 6. Polarized FT-IR spectra of oriented samples with 0° and 90° rotating polarizing angles with respect to the shear direction.

parmolecular hexagonal lattice. This packing scheme is also consistent with the observation of strong (100) diffraction with weak (200) and (110) diffractions. Possible 2*4/1 and 2*6/1 helical chain conformations of vinyl polymers are schematically illustrated in Figure 5b, in which rods and coils represent the phenylene along with ester groups and aliphatic tails in the pendent templates rotating around the helical backbones.

To further examine this packing model in the construction of hexagonal lattice of the orientated samples, polarized FTIR experiments of mechanically sheared samples were conducted, and the results are shown in Figure 6. By rotating the polarizing angle from 0° to 90°, the stretching vibration of carbonyl groups at 1724 cm⁻¹ exhibits a decrease in intensity when the polarized beam is changed from parallel to perpendicular to the shear direction. The dichroic ratio (A_{\parallel}/A_{\perp}) of carbonyl stretching is 1.4. This indicates that the carbonyl stretching direction is essentially parallel to the shear direction (the *c*-axis). The phenylene CH out-of-plane bending at 752 cm⁻¹ is more sensitive to the shear direction, and its dichroic ratio (A_{\parallel}/A_{\perp}) is 2.4. It is deduced that the phenylenes are oriented essentially perpendicular to the shear direction. The methylene and methyl stretching in the region of 2847–2964 cm⁻¹ also exhibits an increase in intensity when the polarized beam is parallel to the shear direction. Using the peak fitting procedure, the stretchings in 2847–2964 cm⁻¹ are separated into five individual peaks at 2847, 2871, 2910, 2934, and 2964 cm⁻¹, and the corresponding dichroic ratios (A_{\parallel}/A_{\perp}) from the integrated area are calculated as 1.4, 1.4, 1.1, 1.5, and 1.4, respectively.



40 μm



40 μm

Shear Direction

Figure 7. PLM morphological observation of the polymer at isothermal temperature of 120 °C (a, top) and uniaxially sheared morphology at 160 °C (b, bottom).

These signals arise from two portions in the polymer structure: one is originated from the polyethylene backbones along the shear direction (the *c*-axis), and the other is from the swallow-tailed 4-heptyl groups. Note that the population of the swallow-tailed 4-heptyl groups is higher than that of the backbones. These dichroic ratios indicate that these groups in the side-chain templates are arrayed more or less perpendicular to the shear direction, which is consistent with our assumption of the helical chain conformation. However, detailed supramolecular arrangement in this hexagonal lattice requires computer simulation, which is currently under investigation.

Finally, PLM observations show that batonnet or focal conic fanlike textures (Figure 7a) are observed at 120 °C for isothermally annealed samples in several minutes after cooling from the isotropic melt at a rate of 2.5 °C/min. This birefringent texture first starts to develop at 190 °C during cooling from the isotropic melt, and it is reproducible in multiple cooling and heating cycles. It is believed that this texture can be identified as a characteristic feature of the supramolecular hexagonal columnar LC phases.²⁴ When the film sample is mechanically sheared at 160 °C, bands with alternating birefringence can be formed, and the band spacing is between 2 and 3 μm, as shown in Figure 7b. The normal direction of these alternative bands is parallel to the shear direction. (The shear direction is indicated by an arrow.) This shear-induced LC banded texture is rec-

ognized as one of the important features of the LC polymers. It is commonly understood that the banded texture can only be formed under an external shear field in low ordered LC phases and two-dimensional columnar phase.^{25–30} Highly ordered smectic and smectic crystal phases are solidlike and, therefore, cannot be mechanically sheared to form these bands.^{27,28} In this case, the WAXD analysis shows that we have a supramolecular columnar phase which possesses a two-dimensional order. The structural formation of these bands is related to a relaxation of oriented viscoelastic LC polymer fluids after the release of external shear fields.^{31–33}

Conclusion

Poly[di(4-heptyl) vinylterephthalate] has been synthesized using a free radical polymerization via a novel monomer, di(4-heptyl) vinylterephthalate. Although this monomer does not possess a LC phase, the resulting polymer apparently exhibits a thermotropic LC behavior. A first-order transition has been found in DSC experiments that possesses a small transition enthalpy, and the transition temperature is cooling rate dependent. WAXD powder experiments indicate that this polymer possesses a supramolecularly ordered structure on a length scale of greater than 1.5 nm. The structural change upon heating and cooling is in agreement with the thermal transitions observed in DSC. Using a WAXD fiber pattern, one-chain hexagonal columnar LC phase can be identified in a two-dimensionally ordered lattice with $a = b = 1.824$ nm and $\gamma = 120^\circ$. The supramolecular packing model has been proposed under an assumption of helical backbone conformations with the slightly tilted alignment of the pendent templates with respect to the ab -plane. This alignment has been further supported by polarized FTIR results. A supramolecular hexagonal columnar LC phase is thus constructed by the self-assembly of the pendent non-mesogenic templates along the aliphatic backbones.

Acknowledgment. The work was supported by CNNSF and the NSF ALCOM Science and Technology Center (DMR-8920147) at Kent State University, Case Western Reserve University, and University of Akron.

References and Notes

- (1) For general references, see e.g.: *Mol. Cryst. Liq. Cryst.* **1988**, 165 (Papers in Honor of the 100th Anniversary of Liquid Crystal Research).
- (2) McArdle, C. B. *Side Chain Liquid Crystal Polymers*; Blackie: Glasgow, 1989.
- (3) Donald, A. M.; Windle, A. H. *Liquid Crystalline Polymers*; Cambridge University Press: Cambridge, 1992.
- (4) Percec, V.; Pugh, C. In ref 2, pp 30–105 and the references therein.
- (5) Shibaev, V. P.; Plate, N. A. *Adv. Polym. Sci.* **1984**, 60/61, 173.
- (6) Hessel, F.; Finkelmann, H. *Polym. Bull.* **1985**, 14, 375.
- (7) Zhou, Q. F.; Li, H. M.; Feng, X. D. *Macromolecules* **1987**, 20, 233.
- (8) Hardouin, F.; Mery, S.; Achard, M. F.; Noirez, L.; Keller, P. *J. Phys. II* **1991**, 1, 511, and Erratum 871.
- (9) Hardouin, F.; Leroux, N.; Mery, S.; Noirez, L. *J. Phys. II* **1992**, 2, 271.
- (10) Leroux, N.; Keller, P.; Achard, M. F.; Noirez, L.; Hardouin, F. *J. Phys. II* **1993**, 3, 1289.
- (11) Arehart, S. V.; Pugh, C. *J. Am. Chem. Soc.* **1997**, 119, 3027.
- (12) Pugh, C.; Shao, J.; Ge, J. J.; Cheng, S. Z. D. *Macromolecules* **1998**, 31, 1779.
- (13) Pugh, C.; Bae, J.-Y.; Dharia, J.; Ge, J. J.; Cheng, S. Z. D. *Macromolecules* **1998**, 31, 4093.
- (14) Zhang, D.; Liu, Y.; Wan, X.; Zhou, Q.-F. *Macromolecules* **1999**, 32, 4494.
- (15) Zhang, D.; Liu, Y.; Wan, X.; Zhou, Q.-F. *Macromolecules* **1999**, 32, 5183.
- (16) Tu, H.; Zhang, D.; Wan, X.; Chen, X.; Zhou, Q.-F. *Macromol. Rapid Commun.* **1999**, 20, 555.
- (17) Yoon, S.; Ichikawa, K.; MacKnight, W. J.; Hsu, S. L. *Macromolecules* **1995**, 28, 5063.
- (18) Schwartz, L. M. *Anal. Chem.* **1971**, 43, 1336.
- (19) Wunderlich, B.; Grebowicz, B. *Adv. Polym. Sci.* **1984**, 60/61, 1.
- (20) Keller, A.; Cheng, S. Z. D. *Polymer* **1998**, 39, 4461.
- (21) Chien, W.; Wunderlich, B. *Macromol. Chem. Phys.* **1999**, 200, 283.
- (22) Ungar, G.; Feijoo, J. L.; Percec, V.; Tound, R. *Macromolecules* **1991**, 24, 953.
- (23) Wunderlich, B. *Macromolecular Physics*; Academic Press: New York, 1973; Vol. I.
- (24) Percec, V.; Tomazos, D.; Heck, J.; Ungar, G. *J. Chem. Soc., Perkin Trans.* **1994**, 2, 38.
- (25) Kerkam, K.; Viney, C.; Kaplan, D. L.; Lombadrdi, S. J. *Nature* **1991**, 349, 596.
- (26) Donald, A. M.; Viney, C.; Windle, A. H. *Polymer* **1983**, 24, 155.
- (27) Yoon, Y.; Zhang, A.; Ho, R.-M.; Cheng, S. Z. D.; Percec, V.; Chu, P. *Macromolecules* **1996**, 29, 294.
- (28) Yoon, Y.; Ho, R.-M.; Moon, B.; Kim, D.; McCreight, K. W.; Li, F.; Harris, F. W.; Cheng, S. Z. D.; Percec, V.; Chu, P. *Macromolecules* **1996**, 29, 3421.
- (29) Ge, J. J.; Zhang, A.; McCreight, K. W.; Ho, R.-M.; Wang, S.-Y.; Jin, X.; Harris, F. W.; Cheng, S. Z. D. *Macromolecules* **1997**, 30, 6498.
- (30) Zheng, R.-Q.; Chen, E.-Q.; Cheng, S. Z. D.; Xie, F.; Yan, D.; He, T.; Percec, V.; Chu, P.; Ungar, G. *Macromolecules* **1999**, 32, 6981.
- (31) Viney, C.; Windle, A. H. *J. Mater. Sci.* **1983**, 18, 1143.
- (32) Hoff, M.; Keller, A.; Windle, A. H. *J. Non-Newtonian Fluid Mech.* **1996**, 67, 241.
- (33) Ge, J. J.; Zhang, J. Z.; Zhou, W.; Li, C. Y.; Jin, S.; Calhoun, B. H.; Wang, S.-Y.; Harris, F. W.; Cheng, S. Z. D. *J. Mater. Sci.*, in press.

MA991768A